

# Critical undeformed chip thickness of brittle materials in single point diamond turning

W. J. Zong<sup>1</sup> · Z. M. Cao<sup>1</sup> · C. L. He<sup>1</sup> · T. Sun<sup>1</sup>

Received: 29 January 2015 / Accepted: 4 May 2015 / Published online: 15 May 2015  
© Springer-Verlag London 2015

**Abstract** In this work, the ultimate compression force that enables the plastic removal of brittle materials in diamond turning is initially modeled according to the theory of rigid-plastic mechanics. And subsequently, an independent oscillator model is reconstructed to calculate the microfriction force that appears at contact interface. As expected, a predictive model considering the ultimate compression force and microfriction force is finally established to calculate the critical undeformed chip thickness of brittle materials in diamond turning, in which a crack-free surface of brittle materials can be achieved as quickly as possible in a brittle-ductile coupled cutting mode. Based on the theoretical predictions and experimental observations, the “size effect” of the critical undeformed chip thickness is discovered, i.e., that the ratio of the critical undeformed chip thickness to tool cutting edge radius increases with the decrement of tool cutting edge radius. Such interesting variation law is attributed to the strengthening of the effect of the microfriction and concentration of the compressive stress under a small enough cutting edge radius, which produces more favorable conditions for the brittle-ductile coupled removal of brittle materials.

**Keywords** Diamond turning · Brittle material · Size effect · Cutting edge radius · Critical undeformed chip thickness

## Nomenclature

$F_p$  Ultimate compressive force due to plastic deformation  
 $F_f$  Microfriction force

$q$  Ultimate compressive stress  
 $k$  Critical yield constant  
 $\gamma$  Half top angle of wedge  
 $\sigma_s$  Yield strength  
 $l_{AB}$  Equivalent interaction length  
 $r_n$  Tool cutting edge radius  
 $r_{n1}$  Equivalent cutting edge radius of tool  
 $\theta$  Half central angle of contact interface  
 $e$  Unit length of cutting edge  
 $\Delta U$  Total deformation energy  
 $\varepsilon$  Specific energy  
 $A_0$  Area of contact interface  
 $\Delta E$  Equilibrium cohesive energy  
 $\gamma_A$  Surface energy of A phase  
 $\gamma_B$  Surface energy of B phase  
 $\gamma_{AB}$  Surface energy of contact interface  
 $E^*[a_k^*]$  Rydberg function  
 $a$  Interface distance  
 $a_0$  Equivalent lattice constant  
 $a_k^*$  Scale lattice constant  
 $a_m$  Equilibrium lattice distance  
 $l$  Scale length  
 $B$  Equilibrium bulk modulus  
 $E$  Young's modulus  
 $\nu$  Poisson's ratio  
 $r_{ws}$  Wigner-Seitz radius  
 $F_n$  Resultant force  
 $\varphi$  Phase angle of resultant force  
 $h_c$  Critical undeformed chip thickness  
 $h_d$  Nominal undeformed chip thickness  
 $l_{BC}$  Length of medial crack  
 $C_m$  Equivalent length of medial crack  
 $\eta$  Constant  
 $\eta_0$  Constant  
 $H$  Vickers hardness

✉ W. J. Zong  
zongwenjun@163.com

<sup>1</sup> Center for Precision Engineering, Harbin Institute of Technology, P.O. Box 413, Harbin 150001, People's Republic of China

|           |                                   |
|-----------|-----------------------------------|
| $Q$       | Indentation load                  |
| $K_{IC}$  | Quasistatic fracture toughness    |
| $K_{ID}$  | Dynamic fracture toughness        |
| $\lambda$ | Tool oblique angle in fly-cutting |

## 1 Introduction

Diamond turning technology is of great importance for the fabrication of precision parts in various industrial sectors, such as optics, clean energy, information and communication technology, and others [1, 2]. It is capable of achieving a super-smooth surface of not only the machinable metals but also the brittle materials, which is free from the conventional time-consuming polishing. The brittle materials, however, are difficult to be machined due to their low fracture toughness and high hardness. Such properties tend to arouse some unwanted fractures, which finally results in a damaged or nontransparent surface as finished. Therefore, in order to achieve a crack-free surface, the topmost surface layer of brittle materials must be removed in ductile mode, in which the critical undeformed chip thickness (CUCT) is usually configured at the submicron scale [3]. In addition to the CUCT, achieving a smooth surface of brittle materials also relies on the machining environment, performance of machine tool, process parameters, tool geometries, cutting edge radius, as well as the properties of workpiece materials [1, 4]. For example, the famous “size effect” of CUCT appears inevitably in diamond turning of brittle materials, and consequently, a lot of cutting trials have to be carried out to optimize the process parameters and tool geometries. It has been demonstrated that the size effect is primarily attributed to the effect of cutting edge radius of diamond tool and the properties of the machined materials [5, 6]. In the light of previous works as reviewed above, interesting questions are raised but not answered satisfactorily: is there an acceptable model that accurately predicts the CUCT of brittle materials in diamond turning coupled with a consideration of size effect? Furthermore, can the prediction model well explain the mechanisms of the size effect-dependent issues?

In order to fulfill the objects, researchers have paid great attention to the fundamental principles and the crucial factors for achieving the ductile regime machining of brittle materials. Liu et al. investigated the effect of tool cutting edge radius on the ductile-brittle transition of chip formation in cutting the silicon wafers [7]. They found that there is a critical undeformed chip thickness in cutting operation, beyond which the chip formation changes from ductile deformation to brittle fracture. In addition, the CUCT depends on tool cutting edge radius. Subsequently, Yan et al. employed the finite element approach to explore the influence of tool cutting edge radius on the cutting forces, flow stress, temperature, as well as chip formation in the submicron-level orthogonal cutting of silicon [8]. They declared that the cutting forces and temperature will

strengthen as tool cutting edge radius increases, which leads to a decrease in the effective cutting depth. To be interesting, the continuous chip formation cannot be realized if tool cutting edge radius is bigger than 500 nm. Arif et al. proposed an analytical model to determine the critical conditions for finishing a crack-free surface on brittle materials by milling process [9, 10]. According to their analysis, if the nominal depth of cut is bigger than the subsurface damage depth, the maximum undeformed chip thickness required in the ductile-mode cutting can be greater than the CUCT for brittle-ductile transition, in which a fracture-free surface is still achievable. However, the CUCT values in their work should be empirically determined in advance. Chen et al. recently carried out many microgrooving experiments on potassium dihydrogen phosphate (KDP) crystals, in which the diamond tool scratches along different crystalline orientations with a low velocity [11]. Their experimental results show that evidence on visible brittle-ductile transition can be found on the bottom of the scratched grooves as the scratching depth increases. Moreover, they also reported that the CUCT strongly depends on the crystalline orientation of KDP crystals.

Furthermore, some interesting hypotheses have also been made to explicate the deformation mechanism of brittle materials in diamond turning. The primary thought is that the microscopic plasticity prevails in the cutting zone as the underformed chip thickness is below to a critical value. This means that the brittle materials in the cutting zone undergo the shearing deformation, being the same distortion as that happens in metal cutting. For example, Bifano et al. put forward a brittle-ductile transition model to interpret the plastic deformation and brittle fracture mechanisms, in which the cutting depth accounting for brittle-ductile transition is considered as a function of intrinsic properties of brittle materials [12]. Venkatachalam et al. proposed a fracture toughness-dependent model to predict the undeformed chip thickness for brittle-ductile transition in diamond turning of brittle materials [13]. Wang et al. found that the specific cutting energy can be considered as a criterion to distinguish the removal mode of hard and brittle materials in scribing process [14]. Cai et al. performed molecular dynamic simulations to represent the nanoscale ductile-mode cutting of monocrystalline silicon. They reported that the ductile-mode removal occurs under two necessary conditions. One is the undeformed chip thickness that is smaller than tool cutting edge radius, and the other is tool cutting edge radius that is below to an upper bound limit. Such requirements are beneficial to produce the high enough hydrostatic pressure in the cutting zone, which suppresses the crack propagation and facilitates the plastic deformation [15]. Arefin et al. investigated the upper bound limit of tool cutting edge radius to make the ductile-mode machining available. They asserted that the upper bound limit for cutting of single crystal silicon wafer is between 700 and 800 nm, and a larger value at the micrometer scale is required

for cutting of tungsten carbide [16]. Arif et al. presented a specific cutting energy-related model to predict the critical condition for brittle-ductile transition in diamond turning of brittle materials, into which the properties of workpiece material, tool geometries, and process parameters are integrated [3]. Subsequently, Zhang et al. modified the specific cutting energy model for the vibration-assisted diamond turning of brittle materials, which further takes the effect of vibration into account [17]. According to the experimental validations on single crystal silicon, they claimed that the vibration-assisted cutting can significantly increase the CUCT of brittle materials. Sun et al. investigated the brittle-ductile transition properties of glass-ceramic and the material removal mechanism by means of nano-indentation, nano-scratching, and Vickers indentation tests. They claimed that the material removal mechanism seems to be directly related to the normal force applied on tool tip and the scratching depth. Below the critical values of applied load and scratch depth, the glass-ceramic can undergo plastic flow rather than brittle fracture [18]. Fang et al. established a model to understand the behavior of material removal in nano-cutting, in which the material removal is attributed to the extrusion of tool edge rather than the conventional shearing deformation. In addition, they also paid great attention to the critical ratio of undeformed chip thickness to tool cutting edge radius. It was found that the critical ratio is dependent on the properties of workpiece material, tool geometry, and machining conditions [19].

Although the interesting works outlined above have made great advances in predicting the CUCT of brittle materials in diamond turning, little attention has paid to the cutting edge radius-dependent size effect of the CUCT, which essentially is a vital factor affecting the brittle-ductile transition property. Therefore, in this work, a novel prediction model is established to calculate the CUCT, into which the size effect is successively integrated. Moreover, microfriction is also considered in the newly developed model, and the constraint conditions for crack propagation in the cutting zone are relaxed as long as the achieving of a crack-free surface is accessible.

## 2 Theoretical modeling

As revealed in previous work, the scratching and diamond turning both produce severe normal pressure and lateral motion on the material surface. Therefore, in this work, the well-established criterion for brittle-ductile transition of brittle materials in scratching process is employed to construct the predictive model for the CUCT in diamond turning. First, the upper boundary limit of force or the ultimate compression force that enables the brittle materials to be removed in plastic deformation is modeled according to the rigid-plastic mechanics theory. Second, an independent oscillator model is reconstructed to calculate the microfriction force at interface

between diamond tool and workpiece, which is of great importance in determining the contact pressure. Finally, a predictive model coupled with the ultimate compression force and microfriction force is established for the CUCT, into which the effects of material properties of workpiece and tool cutting edge radius are successively integrated.

### 2.1 The ultimate compression force in plastic deformation

Figure 1a shows the schematic sketch of material flowing and chip pile-up ahead of tool cutting edge. In this figure,  $\gamma_0$  and  $\alpha_0$  are tool rake and relief angles, respectively.  $h_d$  denotes the nominal cutting thickness. Assume that point B is a critical point on tool cutting edge, below which the materials can be removed in plastic deformation. That is to say,  $h_c$  is the so-called CUCT for brittle-ductile transition. Over point B, the crack propagation prevails, and the materials are dominantly removed in brittle fractures. However, the medial crack can be adjacent to the finished surface as near as possible. Moreover, the brittle workpiece is considered as a rigid-plastic body, and the diamond cutting tool is configured as a rigid body. As the plastic deformation occurs in an ideal rigid-plastic body, the flow stress in the plastic deformation region must comply with the yielding laws, e.g., the famous Tresca or Von Mises criterion. In this work, the 2D cutting model as presented in Fig. 1a is in accord with the plane stress condition, and therefore, the equilibrium condition for the yield stress of material under plastic deformation can be expressed as

$$(\sigma_x - \sigma_y)^2 + 4\tau_{xy}^2 = 4k^2 \quad (1)$$

where  $\sigma_x$  and  $\sigma_y$  are the compressive stresses in  $x$  and  $y$  directions, respectively.  $\tau_{xy}$  is the shear stress, and  $k$  is the critical yield constant.

The critical yield constant  $k$  depends on the material properties, which can be given by

$$k = \begin{cases} \frac{1}{2}\sigma_s, & \text{for Tresca criterion} \\ \frac{1}{\sqrt{3}}\sigma_s, & \text{for Von Mises criterion} \end{cases} \quad (2)$$

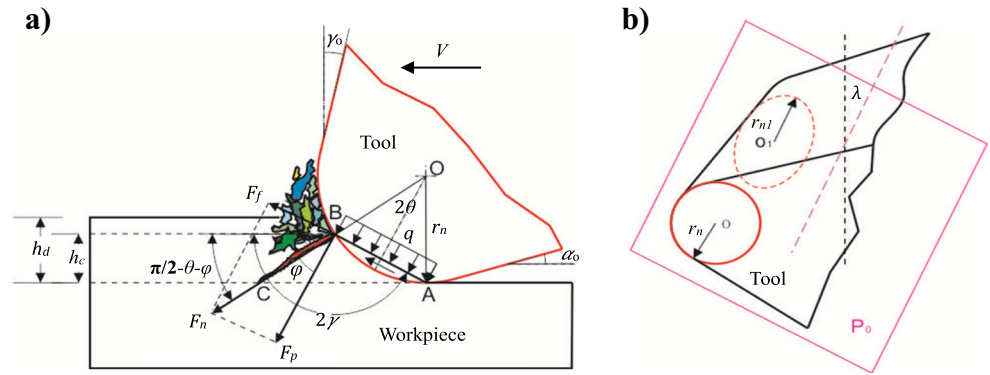
where  $\sigma_s$  is the yielding strength of material.

In rigid-plastic deformation, the stress distribution on tool cutting edge can be simplified into a unilateral compressive wedge model, as schematically presented in Fig. 1a. Therefore, on the basis of slip-line theory, the condition for status switching from plastic deformation to chip separation can be formulated as [20]

$$q = 2k \left( 2\gamma + 1 - \frac{\pi}{2} \right) \quad (3)$$

where  $q$  is the ultimate compressive stress, which is a uniform load distributed on the contact interface.  $2\gamma$  is the top angle of

**Fig. 1** **a** Cutting model for brittle materials in diamond turning; **b** equivalent cutting edge radius of tool



wedge ( $\pi \geq 2\gamma > 0$ ), which determines the loading direction of the ultimate compressive stress  $q$ .

For modeling an ideal unilateral compressive wedge body, the contact region of diamond tool and workpiece is simplified, which is considered as an equivalent straight line between point A and point B. According to the geometrical relationship as shown in Fig. 1a, the length of straight line AB, i.e.,  $l_{AB}$ , can be calculated as

$$l_{AB} = 2r_n \cdot \tan\theta \tag{4}$$

where  $r_n$  is the cutting edge radius of tool and  $2\theta$  is the central angle of contact interface.

The half central angle of contact interface,  $\theta$ , can be worked out in terms of the top angle of wedge  $2\gamma$ , which is given by

$$\theta = \pi - 2\gamma \tag{5}$$

Considering that the contact region is quite small, it is reasonable to assume that the compressive stress induced by diamond tool distributes uniformly on the straight line AB and is perpendicular to it. Therefore, the upper boundary limit of compression force  $F_p$  due to the plastic deformation can be written as

$$F_p(\sigma_s, \theta, r_n, e) = q \cdot l_{AB} \cdot e \tag{6}$$

where  $e$  is the unit length of cutting edge.

### 2.2 Microfriction force

In diamond turning of brittle materials, the cutting parameters are always configured to yield extremely small undeformed chip thickness, and the order of which is comparable to the lattice size of materials as machined. In this case, the size effect appears, and the effect of microfriction force between diamond tool and workpiece becomes more significant, which in return heavily affects the material removal. Therefore, the equivalent crystal theory (ECT) [21, 22] is introduced in this work to reveal the influence of microfriction force in diamond turning of brittle materials. By considering the relationship between the energy and location of atoms, ECT has been widely applied to

explore the effect of microfriction and explain the formation mechanisms of nascent surface and defect in semiconductors and metal crystals. According to the principle of ECT, an independent oscillator (IO) model [23, 24] coupled with the effect of tool cutting edge radius, material properties of workpiece, and their interactions is first proposed in this work to calculate the microfriction force,  $F_f$ , which is formulated as

$$F_f = \frac{\Delta U}{a_0} \tag{7}$$

where  $a_0$  is the equivalent lattice constant of material, and  $\Delta U$  is the total energy consumed in generating defects or nascent surface.

The total energy  $\Delta U$  for a deformable body can be given by

$$\Delta U = A_0 \cdot \varepsilon = A_0 \cdot \sum \varepsilon_i \tag{8}$$

where  $A_0$  is the area of contact interface of two bodies, and  $A_0 \approx l_{AB} \cdot e$  in this work.  $\varepsilon$  is the specific energy as required for producing defects or nascent surface, and  $\varepsilon_i$  is the contribution of atom  $i$  adjacent to the defects or nascent surface to the energy consumption.

In a real atom system, many body terms will contribute to the energy of each atom. That is to say,  $\varepsilon_i$  can be written as a group of perturbation series of many body terms, and each of which is considered as a collection of various equivalent single crystal [21]. Therefore, the calculation of  $\varepsilon_i$  can be expressed as

$$\varepsilon_i = \Delta E \cdot \sum_{i=1}^4 (1 + E^*[a_k^*(i)]) \tag{9}$$

where  $E^*[a_k^*(i)]$  is the Rydberg function to represent the universal energy relation.  $\Delta E$  is the equilibrium cohesive energy of individual atom.  $a_k^*$  is the scale lattice constant.

Then,  $\Delta E$  can be calculated according to the surface energies of two contact bodies, which is given by

$$\Delta E = \gamma_A + \gamma_B - \gamma_{AB} \tag{10}$$

where  $\gamma_A$  and  $\gamma_B$  are the surface energies of contact bodies A and B, respectively.  $\gamma_{AB}$  is the equivalent surface energy of contact interface between bodies A and B.

If the contact bodies A and B are the same material,  $\gamma_{AB}$  equals to the sum of the surface energies of phase A and phase B. If the contact bodies A and B are different materials, and the atoms of them can diffuse with each other,  $\gamma_{AB}$  is approximately calculated as follows:  $\gamma_{AB} \approx 0.25(\gamma_A + \gamma_B)$ . If the contact bodies A and B are different materials, and the atoms of them have no access to mutual diffusion,  $\gamma_{AB}$  is formulated as  $\gamma_{AB} \approx 0.75(\gamma_A + \gamma_B)$ .

Moreover, the Rydberg function  $E^*[a_k^*]$  is calculated as

$$E^*[a_k^*] = -(1 + a_k^*) \exp(-a_k^*) \tag{11}$$

where  $E^*[a_1^*]$  is the contribution of single body term to energy consumption as required in defects or nascent surface formation, which can be considered as the variation of localized atom density.  $E^*[a_2^*]$  is the contribution of two-body terms that is responsible for the energy increase due to the compression of atom bonds.  $E^*[a_3^*]$  is the contribution of three-body terms that accounts for the energy increase due to the distortion of atom bond angles.  $E^*[a_4^*]$  is the contribution of four-body terms to describe the face diagonal anisotropy [25].

In this work, the workpiece is regarded as a rigid body. Therefore,  $\varepsilon_i$  is primarily determined by the effect of single body term  $E^*[a_1^*]$ , and the contributions of many body terms, including  $E^*[a_2^*]$ ,  $E^*[a_3^*]$ , and  $E^*[a_4^*]$ , are all equal to zero.

The scale lattice constant  $a_k^*$  is a function of the interface distance  $a$  and the equilibrium lattice distance  $a_m$ , which is expressed as

$$a_k^* = \frac{(a - a_m)}{l} \tag{12}$$

where  $(a - a_m)$  is approximate to  $0.207a_0$  for the face-centered cubic (fcc) and body-centered cubic (bcc) crystals, and  $l$  is the scale length.

The scale length  $l$  is written as

$$l = 2 \cdot \left( \frac{\Delta E}{12 \cdot \pi \cdot B \cdot r_{ws}} \right)^{1/2} \tag{13}$$

where  $B$  is the equilibrium bulk modulus of crystal material, and  $r_{ws}$  is the Wigner-Seitz radius:  $r_{ws} \approx 0.3908a_0$  for the fcc crystals, and  $r_{ws} \approx 0.4924a_0$  for the bcc crystals [26].

The equilibrium bulk modulus  $B$  of crystal materials is given by

$$B = \frac{E}{3 \cdot (1 - 2\nu)} \tag{14}$$

where  $E$  and  $\nu$  are the Young’s modulus and Poisson’s ratio of crystal materials, respectively.

### 2.3 Modeling on the CUCT

Based on the plastic deformation mechanism, the ultimate compression force  $F_p$  and microfriction force  $F_f$  in diamond turning of brittle materials have been successively modeled in above sections, which take the material properties of work-piece, cutting edge radius of diamond tool, and interactions at contact interfaces into account. In order to solve the CUCT, i.e.,  $h_c$  as shown in Fig. 1a, the composition of forces  $F_p$  and  $F_f$  is further fulfilled at the critical point B, which can be expressed as

$$\begin{cases} F_n = \sqrt{F_p^2 + F_f^2} \\ \varphi = \arctan\left(\frac{F_f}{F_p}\right) \end{cases} \tag{15}$$

where  $F_n$  is the resultant force and  $\varphi$  is defined as the phase angle of resultant force  $F_n$ , which denotes the loading direction of resultant force  $F_n$ .

As well known for the brittle materials, indentation test is an effective method to determine the threshold conditions for brittle-ductile transition or the important material parameters, such as the fracture toughness, hardness, elastic modulus, as well as the other performances, by analyzing the crack state, applied load, and indentation depth. In this work, Vickers indentation is suggested to determine the material properties for modeling the CUCT, which can provide small enough estimation errors by using a pyramid diamond indenter. In Vickers indentation test, the quasistatic fracture toughness of indented brittle materials,  $K_{IC}$ , is calculated as [27]

$$K_{IC} = \eta \cdot \left(\frac{E}{H}\right)^{1/2} \cdot \frac{Q}{C_m^{3/2}} \tag{16}$$

where  $H$  is the Vickers hardness.  $\eta$  is a coefficient, which is configured as  $0.016 \pm 0.004$ .  $Q$  is the applied load or indention force, and  $C_m$  is the equivalent length of medial crack.

Moreover, three assumptions should be made. The first is that the critical point B is equivalent to the tip of Vickers indenter, at which the propagation of median crack is triggered. The second is that the propagation direction of median crack or indention force  $Q$  is the same as the loading direction of resultant force  $F_n$ . The third is that the area of contact interface  $A_0$  is approximate to one fourth of the contact area in Vickers indentation, i.e.,  $Q \approx 4 \cdot F_n$ .

According to the assumptions above, the equivalent length of medial crack  $C_m$  can be given by

$$C_m = \left[ \eta_0 \cdot \left(\frac{E}{H}\right)^{1/2} \cdot \frac{F_n}{K_{ID}} \right]^{2/3} \tag{17}$$

where  $\eta_0$  is the constant in relation to the dynamic effects, and the experimental data presented later suggest empirically that

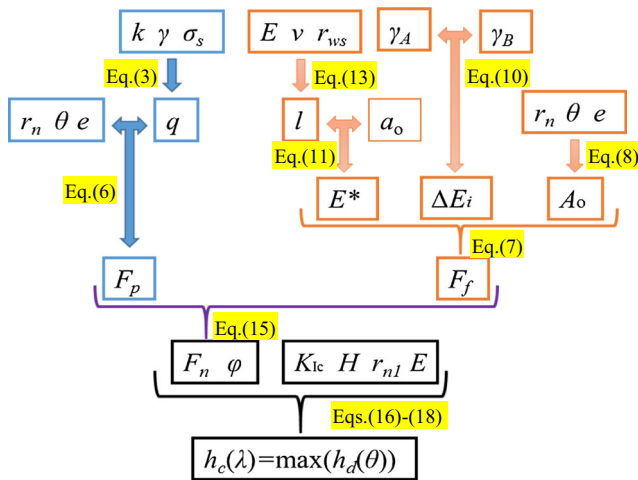


**Fig. 2** Solution procedures for the CUCT of brittle materials in diamond turning

$\eta_0$  is set as  $0.007 \pm 0.0005$ .  $K_{ID}$  is the dynamic fracture toughness, which can be valued as 60–70 % of  $K_{IC}$  for the ductile materials and 30 % or even less of  $K_{IC}$  for the brittle materials.

In order to get a higher removal rate, the constraint condition for the CUCT is relaxed in this work, i.e., that the undeformed chip can be removed in plastic deformation and fracture coupled mode as long as a crack-free surface can be finished in diamond turning. This means that the medial crack propagation can be close to the machined surface as near as possible until the condition of  $l_{BC} = C_m$  is reached.

Therefore, the nominal undeformed chip thickness  $h_d$  that corresponds to the brittle-ductile coupled removal of brittle materials can be expressed as

$$h_d(\theta, r_n) = l_{BC} \cdot \sin\left(\frac{\pi}{2} - \theta - \varphi\right) = l_{BC} \cdot \cos(\theta + \varphi) \quad (18)$$

For a selected diamond tool, the cutting edge radius  $r_n$  is an invariable parameter, and hence, the limit of nominal

undeformed chip thickness  $h_d$  can reach up to the CUCT, i.e.,  $\max(h_d(\theta)) = h_c$ .

In order to validate the CUCT model as developed above, a lot of oblique fly-cutting experiments are performed in this work, in which the diamond tool can be rotated through an indexing fixture to generate different inclination angles of rake face. Therefore, the cutting edge radius is regarded as a function of the oblique angle in cutting, as schematically presented in Fig. 1b. Here, the equivalent cutting edge radius  $r_{n1}$  is proposed for the oblique fly-cutting validations, which can be written as

$$r_{n1} = \frac{r_n}{\cos \lambda} \quad (19)$$

where  $\lambda$  is the oblique angle in fly-cutting.

Finally, all the related analysis procedures to solve the CUCT of brittle materials in diamond turning are summarized in Fig. 2.

### 3 Experimental procedure

In order to validate the newly developed CUCT model, the oblique fly-cutting experiments are carried out on a home-made machine tool, as shown in Fig. 3, which is equipped with a high accuracy air spindle and has a rotation run-out of less than 30 nm. A rounded diamond tool is employed as the fly-cutter, and the rake and flank faces of which are both oriented as the (100) crystal plane, i.e., that the surface energy of tool  $\gamma_B$  is equal to  $9.2 \text{ J/m}^2$ . Tool nose radius is designed as 0.5 mm, and the rake and relief angles are  $0^\circ$  and  $9^\circ$ , respectively. The measured cutting edge radius  $r_n$  of diamond tool is 175 nm, which is evaluated directly by an atomic force microscope (AFM), i.e., the Nanite B supplied by Nanosurf Ltd. AFM operations for measuring the cutting edge radius can be found in our previous work [28]. Some

**Fig. 3** Experimental setup as employed in oblique fly-cutting

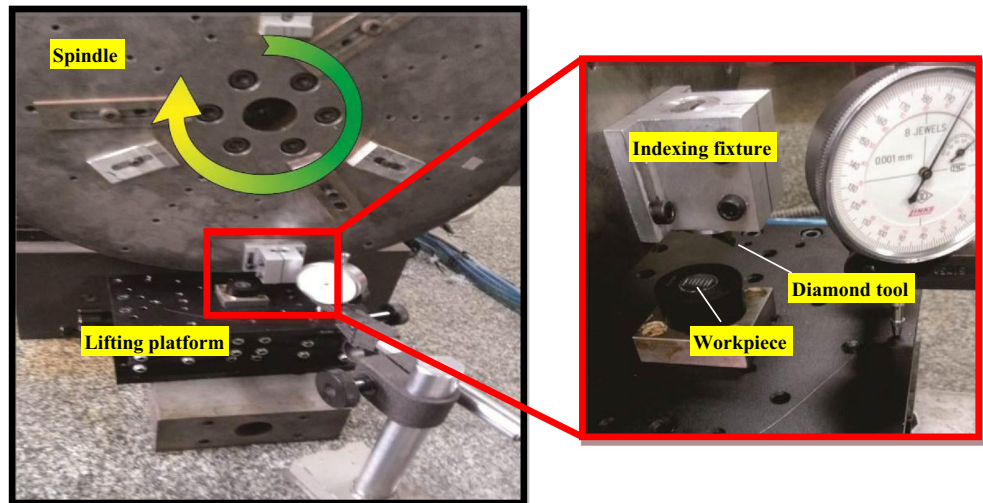


**Table 1** Material properties of workpiece [29]

| $\sigma_s$ [MPa] | $a_o$ [nm] | $\gamma_A$ [J/m <sup>2</sup> ] | $E$ [GPa] | $\nu$ | $HV$ [kg/mm <sup>2</sup> ] | $K_{IC}$ [MPa <sup>2</sup> m <sup>1/2</sup> ] |
|------------------|------------|--------------------------------|-----------|-------|----------------------------|---|
| 43.98            | 0.541      | 5.0                            | 90.438    | 0.3   | 200                        | 1.13  |

polished Cleantran ZnS substrates (fcc crystals) are employed as the tested brittle workpieces, and the material properties of which are given in Table 1.

Before any oblique fly-cutting test, diamond tool should be adjusted through the indexing fixture according to the assigned oblique angle  $\lambda$ . Meanwhile, the workpiece is raised slowly by controlling a lifting platform, through which the tool edge can approach the topmost surface of workpiece as near as possible. And subsequently, the workpiece is raised again to realize the maximal depth of cut as designed for fly-cutting. After the completion of oblique fly-cutting, the scratched slots are also measured with the Nanite B AFM, and the observed critical depths in relation to the appearance of brittle fractures at the cut-in and cut-out positions are employed to calculate the average CUCT.

## 4 Results and discussion

### 4.1 Critical undeformed chip thickness

Figure 4 shows the cut-in and cut-out topographies of slots that scratched under different oblique angles and 2D profiles sampled to read the critical depth for brittle removal, i.e., the CUCT. From the illustrations in Fig. 4, an evident transition from ductile-cutting to brittle-cutting can be observed on the slot bottom with the increase of cutting depth. In the ductile-cutting region, the bottom surface of slot is as smooth as the originally polished surface. In the brittle cutting region, however, the scratched surface is rugged, and the crack propagation induced pits distribute randomly on the slot bottom. According to the boundary of brittle-cutting and ductile-cutting, the critical

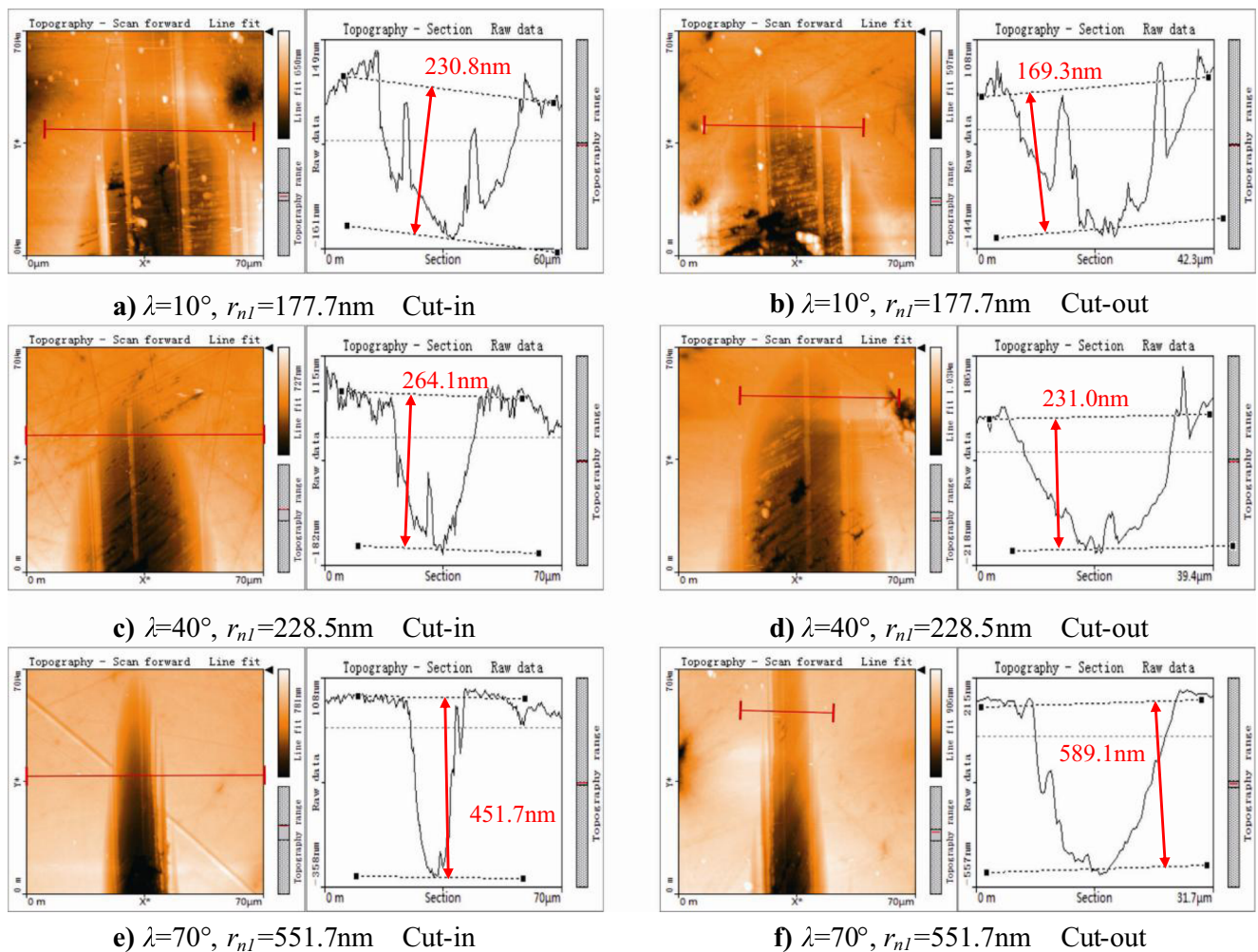


**Fig. 4** Cut-in and cut-out topographies of slots produced under different oblique angles and the corresponding 2D profiles captured for reading the CUCT

**Table 2** CUCTs obtained in experiment and in prediction

| Test no. | $\lambda$ [°] | $r_{n1}$ [nm] | $h_c$ [nm] |         |         |           |         |
|----------|---------------|---------------|------------|---------|---------|-----------|---------|
|          |               |               | Cut-in     | Cut-out | Average | Predicted | Error   |
| 01       | 0             | 175.00        | 170.30     | 183.70  | 177.00  | 198.31    | 12.04 % |
| 02       | 5             | 175.67        | 181.40     | 202.20  | 191.80  | 198.81    | 3.65 %  |
| 03       | 10            | 177.70        | 230.80     | 169.30  | 200.05  | 200.34    | 0.14 %  |
| 04       | 15            | 181.17        | 209.00     | 179.50  | 194.25  | 202.94    | 4.47 %  |
| 05       | 20            | 186.23        | 206.90     | 213.20  | 210.05  | 206.70    | 1.59 %  |
| 06       | 25            | 193.09        | 256.40     | 217.50  | 236.95  | 211.75    | 10.64 % |
| 07       | 30            | 202.07        | 225.20     | 162.70  | 193.95  | 218.26    | 12.54 % |
| 08       | 35            | 213.64        | 253.60     | 165.00  | 209.30  | 226.51    | 8.22 %  |
| 09       | 40            | 228.45        | 264.10     | 231.00  | 247.55  | 236.86    | 4.32 %  |
| 10       | 45            | 247.48        | 306.00     | 283.10  | 294.55  | 249.85    | 15.18 % |
| 11       | 50            | 272.25        | 221.40     | 239.40  | 230.40  | 266.25    | 15.56 % |
| 12       | 55            | 305.10        | 258.60     | 301.90  | 280.25  | 287.26    | 2.50 %  |
| 13       | 60            | 350.00        | 394.70     | 354.20  | 374.45  | 314.79    | 15.93 % |
| 14       | 65            | 414.09        | 577.40     | 529.90  | 553.65  | 352.13    | 36.40 % |
| 15       | 70            | 511.67        | 451.70     | 589.10  | 520.40  | 405.48    | 22.08 % |
| 16       | 75            | 676.15        | 394.20     | 441.50  | 417.85  | 488.28    | 16.86 % |
| 17       | 80            | 1000.78       | 696.20     | 573.00  | 634.60  | 637.12    | 0.40 %  |

depth or the CUCT can be acquired directly from the 2D profiles that captured at the cut-in and cut-out positions.

From the CUCT variations in Fig. 4, it can be found that the sampled CUCT increases with the increment of tool oblique angle. Such variation law can be well explained by the newly developed prediction model in this work. As indicated by Eq. (19), the increment of tool oblique angle will enlarge the equivalent cutting edge radius, which in return increases the length of wedge body  $l_{AB}$  in terms of Eq. (4). As revealed by Eqs. (7) and (8), the increase of  $l_{AB}$  leads to the enlargement of contact interface area, which finally results in the enhancement of microfriction force. As pictorially shown in Fig. 1a, the increase of microfriction force will change the direction of medial crack propagation, i.e., that the medial crack propagation inclines toward the unmachined surface. Therefore, although the increment of tool oblique angle makes the medial crack become longer, the inclination of medial crack propagation to the unmachined surface resultantly increases the CUCT.

Moreover, it can also be found in Fig. 4 that there are some differences in the CUCT sampled at the cut-in and cut-out positions under the same tool oblique angle. This may be due to the variation of crack propagation caused by the inclination of the ultimate compressive stress distribution. Therefore, the average value of the CUCTs sampled at the cut-in and cut-out positions is considered as the final output result in experiment. All the results in experiment and in theory are listed in Table 2 and presented in Fig. 5a, in which the prediction error is calculated as

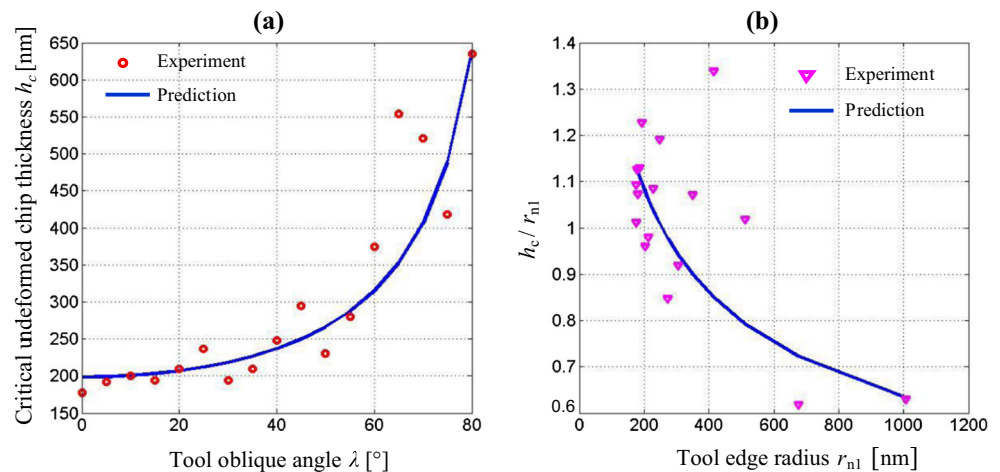
$$error = \left| \frac{h_{c-measured} - h_{c-predicted}}{h_{c-measured}} \right| \times 100\% \quad (20)$$

It can be seen clearly from Table 2 and Fig. 5a that the predicted results have a good consistency with the experimental data, although the equivalent tool cutting edge radius  $r_{n1}$  considerably varies in the previous 13 groups of experiments. More importantly, the maximal prediction error is only 15.93 %, which well validates the theoretical prediction model as established for the CUCT of brittle materials in this work. In the following four trials, however, the prediction errors are relatively high, which may result from a bigger tool oblique angle leading to a greater deviation of the equivalent cutting edge radius  $r_{n1}$  as calculated with Eq. (19). In addition, some reasons out of the assumptions for the theoretical modeling should not be neglected too, such as the dynamic impact in fly-cutting, microscopic defects in the bulk of brittle materials, and measurement errors. However, as reported in previous work, the size effect owing to the influence of tool cutting edge radius must be an important reason for this inconsistency, which will be discussed in detail in the following section.

#### 4.2 Size effect of the CUCT

Size effect of the CUCT has been clearly demonstrated in Fig. 5b, i.e., the variation law of the ratio of  $h_c/r_{n1}$  to tool cutting edge radius  $r_{n1}$ . As shown in Fig. 5b, the values of  $h_c/r_{n1}$  in experiment and in prediction both decrease with the increasing of  $r_{n1}$ . While  $r_{n1}$  is equal to 350 nm, a relatively large inconsistency appears between the  $h_c/r_{n1}$  in experiment and that in prediction, such as the last five data as listed in Table 2. More interestingly, once  $r_{n1}$  is

**Fig. 5** Verification and analysis for the developed CUCT model; **a**  $h_c$  obtained in prediction and in experiment; **b** variations of  $h_c/r_{n1}$  vs tool cutting edge radius  $r_{n1}$



larger than 350 nm, as shown in Fig. 5b, the differences of  $h_c/r_{n1}$  in experiment and in prediction become more visible. In particular, as  $r_{n1}$  approaches 414.09 nm, the differences reach the maximal, which corresponds to the maximum prediction error of 36.40 %, as presented in Table 2. These random characteristics of CUCT as observed above are attributed to the appearance of random brittle fractures and unpredictable propagation direction of medial crack caused by the increment of tool cutting edge radius. In the case of  $r_{n1} > 350$  nm, the effects of extrusion and friction become dominant in the material removal procedure. Because of the enlargement of tool cutting edge radius, however, the contact area increases at the same time. Finally, the compressive stress on the contact interface will reversely decrease. That is to say, the distribution of compressive stress on the contact interface under a large tool cutting edge radius may be out of the assumptions of plastic deformation for Eq. (1), which deteriorates the brittle-ductile coupled removal mode and leads to the great fluctuations of CUCT as revealed in Fig. 5b and Table 2.

Moreover, it can also be found from Fig. 5b that the ratio of  $h_c/r_{n1}$  varies from 0.62 to 1.34 and increases with a decreasing in tool cutting edge radius. Such interesting observation validates again that in diamond turning of brittle materials, the microfriction becomes a significant factor affecting the CUCT. As revealed in previous work, the material removal mode is heavily dependent on tool cutting edge radius [30]. In Fig. 5b, it can also be found that the scratching and ploughing gradually account for the dominant removal mode of materials as tool cutting edge radius decreases step by step, which strengthens the effect of the microfriction in the contact region. In addition, the decrement of tool cutting edge radius causes the decrease of contact area as indicated by Eq. (4). As a result, the compressive stress concentrates more and more on the decreasing contact area, which produces more favorable conditions for the

plastic deformation of brittle materials. Therefore, as pictorially presented in Fig. 5b, the ratio of  $h_c/r_{n1}$  will reversely increase with a decrement of tool cutting edge radius, which is named the size effect of CUCT in this work.

## 5 Conclusions

In this work, the important factors affecting the critical undeformed chip thickness of brittle materials in diamond turning are analyzed systematically, and a novel model is finally formulated to predict the critical undeformed chip thickness. More interestingly, the size effect of the critical undeformed chip thickness is first observed and explained according to the newly developed model. In terms of the presented results and discussions above, some important conclusions can be drawn as follows:

- (1) The ultimate compression force that enables the brittle materials to be removed in ductile mode is modeled according to the theory of rigid-plastic mechanics. And subsequently, an independent oscillator model is reconstructed to calculate the microfriction force that appears at the interface between diamond tool and workpiece. In such a way, a predictive model coupled with the ultimate compression force and microfriction force is successively established to calculate the critical undeformed chip thickness of brittle materials in diamond turning, which can give a satisfied consistency with the experimental observations.
- (2) The critical undeformed chip thickness of brittle materials in diamond turning depends upon the material properties, tool cutting edge radius, and the dynamic interaction between diamond tool and workpiece. In addition, the size effect is also a quite significant factor. With the decrement of tool cutting edge radius, the ratio of the

critical undeformed chip thickness to tool cutting edge radius presents an increasing trend. This is due to the strengthening of the effect of the microfriction and concentration of the compressive stress, which produces more favorable conditions for the brittle-ductile coupled removal of brittle materials.

**Acknowledgments** The authors would like to thank the National Natural Science Foundation of China for the support of this work (No. 51175127). Furthermore, this work was supported by the Fundamental Research Funds for the Central Universities (No. HIT.BRETHIII.201412) and the Major Special Subject of High-end CNC Machine Tools and Basic Manufacturing Equipment Science and Technology of China (No. 2011ZX04004-031). Furthermore, the authors would sincerely thank the reviewers for their very professional suggestions on this work.

## References

- Ikawa N, Donaldson RR, Komanduri R, König W, McKeown PA, Moriwaki T, Stowers IF (1991) Ultraprecision metal cutting—the past, the present and the future. *CIRP Ann Manuf Technol* 40(2):587–594
- Son SM, Lim HS, Ahn JH (2005) Effects of the friction coefficient on the minimum cutting thickness in micro cutting. *Int J Mach Tool Manuf* 45(4):529–535
- Arif M, Zhang XQ, Rahman M, Kumar S (2013) A predictive model of the critical undeformed chip thickness for ductile–brittle transition in nano-machining of brittle materials. *Int J Mach Tool Manuf* 64:114–122
- Dornfeld D, Min S, Takeuchi Y (2006) Recent advances in mechanical micromachining. *CIRP Ann Manuf Technol* 55(2):745–768
- de Oliveira FB, Rodrigues AR, Coelho RT, de Souza AF (2015) Size effect and minimum chip thickness in micromilling. *Int J Mach Tool Manuf* 89:39–54
- Woon KS, Rahman M (2010) The effect of tool edge radius on the chip formation behavior of tool-based micromachining. *Int J Adv Manuf Technol* 50(9–12):961–977
- Liu K, Li XP, Rahman M, Neo KS, Liu XD (2007) A study of the effect of tool cutting edge radius on ductile cutting of silicon wafers. *Int J Adv Manuf Technol* 32(7–8):631–637
- Yan J, Zhao H, Kuriyagawa T (2009) Effects of tool edge radius on ductile machining of silicon: an investigation by FEM. *Semicond Sci Technol* 24(7):075018
- Arif M, Rahman M, San WY (2011) Analytical model to determine the critical feed per edge for ductile-brittle transition in milling process of brittle materials. *Int J Mach Tool Manuf* 51(3):170–181
- Arif M, Rahman M, San WY (2012) Analytical model to determine the critical conditions for the modes of material removal in the milling process of brittle material. *J Mater Process Technol* 212(9):1925–1933
- Chen HF, Zheng ZW, Dai YF, Gao H, Li XP (2010) Critical undeformed chip thickness and cutting pressure in relation to ductile mode cutting of KDP crystal. *Key Eng Mater* 443:582–587
- Bifano TG, Dow T, Scattergood R (1991) Ductile-regime grinding: a new technology for machining brittle materials. *J Manuf Sci Eng* 113(2):184–189
- Venkatachalam S, Li X, Liang SY (2009) Predictive modeling of transition undeformed chip thickness in ductile-regime micro-machining of single crystal brittle materials. *J Mater Process Technol* 209(7):3306–3319
- Wang J-J, Liao Y-Y (2008) Critical depth of cut and specific cutting energy of a microscribing process for hard and brittle materials. *J Eng Mater Technol* 130(1):011002
- Cai M, Li X, Rahman M (2007) Study of the mechanism of nanoscale ductile mode cutting of silicon using molecular dynamics simulation. *Int J Mach Tool Manuf* 47(1):75–80
- Arefin S, Li X, Rahman M, Liu K (2007) The upper bound of tool edge radius for nanoscale ductile mode cutting of silicon wafer. *Int J Adv Manuf Technol* 31(7–8):655–662
- Zhang XQ, Arif M, Liu K, Kumar AS, Rahman M (2013) A model to predict the critical undeformed chip thickness in vibration-assisted machining of brittle materials. *Int J Mach Tool Manuf* 69:57–66
- Sun YL, Zuo DW, Wang HY, Zhu YW, Li J (2011) Mechanism of brittle-ductile transition of a glass-ceramic rigid substrate. *Int J Miner Metal Mater* 18(2):229–233
- Fang FZ, Wu H, Liu YC (2005) Modelling and experimental investigation on nanometric cutting of monocrystalline silicon. *Int J Mach Tool Manuf* 45(15):1681–1686
- Xia ZG (2005) Plastic mechanics theory. Tongji University Press, Shanghai (in chinese)
- Smith J, Perry T, Banerjee A, Ferrante J, Bozzolo G (1991) Equivalent-crystal theory of metal and semiconductor surfaces and defects. *Phys Rev B* 44(12):6444–6465
- Ferrante J, Zypman FR (2006) Generalization of equivalent crystal theory to include angular dependence. *Comput Mater Sci* 36(4):425–431
- Tomlinson GA (1929) CVI. A molecular theory of friction. *Lon Edin Dub Phil Mag J Sci* 7(46):905–939
- Ding LY, Huang P (2010) Study of interfacial friction mechanism based on the coupled-oscillator model. *Wear* 268(1):172–177
- Aghemenloh E, Idioudi JOA, Azi SO (2009) Surface energies of hcp metals using equivalent crystal theory. *Comput Mater Sci* 46(2):524–530
- Ren F, Cao K, Ren J, Volinsky AA, Tran TH, Tian B (2014) Numerical calculation of the electron density at the Wigner–Seitz radius based on the thomas-fermi-dirac equation. *J Comput Theor Nanosci* 11(2):344–347
- Cheng X, Wei XT, Yang XH, Guo YB (2014) Unified criterion for brittle–ductile transition in mechanical microcutting of brittle materials. *J Manuf Sci Eng* 136(5):051013
- Zong WJ, Li ZQ, Sun T, Cheng K, Li D, Dong S (2010) The basic issues in design and fabrication of diamond-cutting tools for ultra-precision and nanometric machining. *Int J Mach Tool Manuf* 50(4):411–419
- Yu HZ (2007) Infrared optical materials. National Defense Industry Press, Beijing (in chinese)
- Zong WJ, Huang YH, Zhang YL, Sun T (2014) Conservation law of surface roughness in single point diamond turning. *Int J Mach Tool Manuf* 84:58–63